

AD-A009 208

A CALCULATIONAL MODEL FOR HIGH
ALTITUDE EMP

Louis W. Seiler, Jr.

Air Force Institute of Technology
Wright-Patterson Air Force Base, Ohio

March 1975

DISTRIBUTED BY:

NTIS

National Technical Information Service
U. S. DEPARTMENT OF COMMERCE

Abstract

An electromagnetic pulse (EMP) model is developed which allows a quick computation of the time development of the electric fields generated by a high altitude nuclear burst. The model is based on the Karzas-Latter high frequency approximation for high altitude EMP, which describes fields generated by Compton electrons interacting with the earth's magnetic field. The proper choice of a gamma time output function, which can be integrated in closed form, and a small angle approximation, made in the expressions for the Compton currents and air conductivity, eliminate the time consuming numerical integrations usually necessary in EMP models to compute the Compton currents and air conductivity. This results in a considerable savings in computation time. The model is presented in a manner which is simple to use but still allows the variation of the major theoretical parameters in the problem.

A simplified model of electron collision frequency as a function of electric field strength is given which enables the model to predict accurate results for nuclear weapon gamma yields up to at least 100 Kt. The results predicted by this EMP model compare to within 5.5% with results from the Air Force Weapons Laboratory CHEMP computer code.

The computation time using the presented model on a CDC 6600 computer is typically 5 sec or less for a 5 shake computation period in steps of .1 shake.

The model presented should be useful for both classroom instruction and nuclear vulnerability/survivability studies and analysis problems.

II. Theory

Overview

Since the solution to the EMP problem is actually the solution of a classical electromagnetic theory problem, the derivation of the model equations reduces to putting Maxwell's equations into a convenient form. This is essentially accomplished by expressing Maxwell's equations in spherical coordinates and transforming to a retarded time frame. One must also develop expressions for the currents and conductivities of the system in the absorption region. The general equations describing the high altitude model of Karzas and Latter have been derived in great detail by Chapman (Ref 3). Only the major points of the derivation will be given here. The system origin is assumed to be at the burst point with detonation at time $t = 0$. This geometry is illustrated in Fig. 1.

The key points to be remembered in this model are:

1. Each gamma ray gives rise to one downward traveling Compton electron.
2. The electrons are turned by the earth's magnetic field giving rise to a centrifugal acceleration.
3. The relativistic electrons radiate energy in their forward direction.
4. The gamma rays and the EMP radiation travel at the same speed. This leads to constructive interference of the radiation from each of the electrons.

Particle Densities

The gamma rays from the nuclear weapon travel in a straight line to a point where they produce Compton electrons. At any given point r

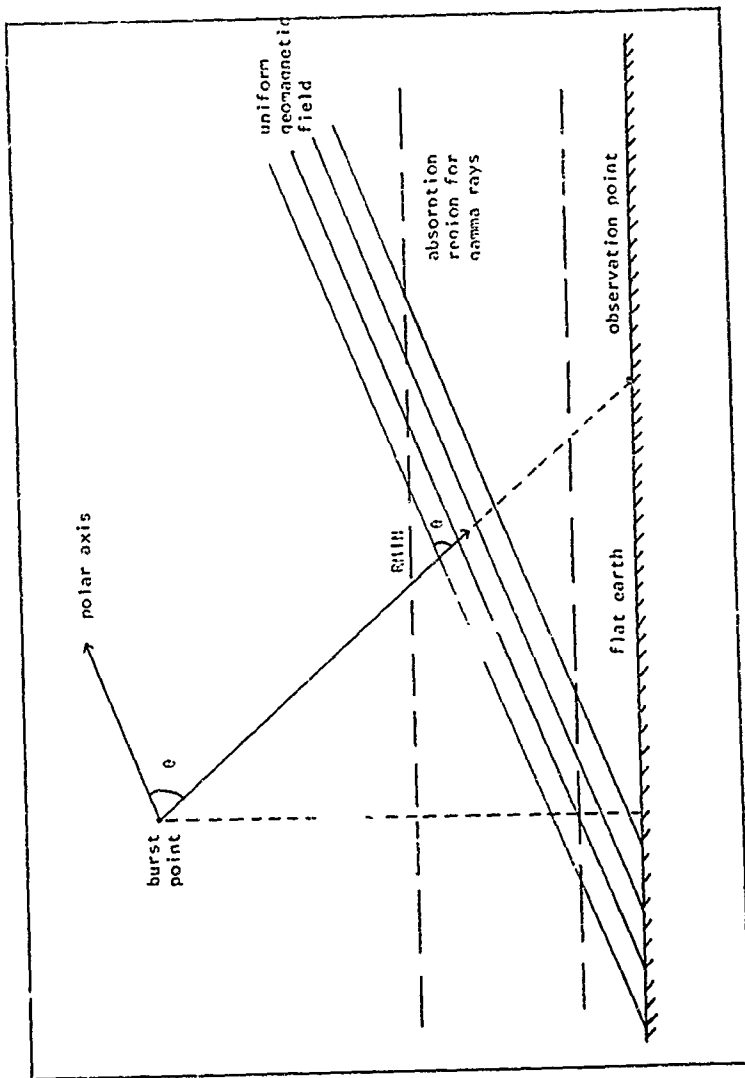


Fig. 1. Model Geometry

the number of gammas which interact to produce Compton electrons is

$$g(r) = \frac{Y}{E} \frac{\exp \left[- \int_0^r \frac{dr'}{\lambda(r')} \right]}{4\pi r^2 \lambda(r)} \quad (1)$$

where $\lambda(r)$ is the mean free path of gamma rays to produce Compton electrons, Y is the gamma yield of the weapon in electron volts (eV), and E is the mean gamma energy in eV.

Equation (1) may also be called the radial distribution function, or an attenuation function for interacting gamma rays. The $\frac{Y}{E}$ term is the total number of gamma rays available from the weapon. The $4\pi r^2$ term accounts for the divergence of the gamma rays as the radius r is increased while the remaining terms account for the reduction in gammas due to their absorption in the atmosphere, based on the mean free path.

It is assumed that the gamma mean free path varies as the exponential atmosphere. This gives the functional relationship between λ and r :

$$\lambda(r) = \lambda_0 \exp \{ (HOB - r \cos A) / S \} \quad (2)$$

where

λ_0 = gamma mean free path at standard pressure

HOB = height of burst in km above the earth's surface

r = radial distance from the burst point to the point of interest

A = angle between the position vector \vec{r} and the vertical

S = atmospheric scale height

With this assumption, Eq (1) can be integrated and becomes

$$g(r) = \frac{Y}{E} \frac{1}{4\pi r^2 \lambda(r)} \exp \left\{ - \frac{S}{\lambda_0 \cos A} \exp \left(- \frac{HOB}{S} \right) \left[\exp \left(\frac{r \cos A}{S} \right) - 1 \right] \right\} \quad (3)$$

Now if $f(t)$ is the time distribution function of the weapon yield, the rate of Compton electrons, n_c , produced at a given point r and time t is given by

$$\frac{dn_c}{dt} = g(r) f\left(t - \frac{r}{c}\right) \quad (4)$$

Each Compton electron produces through inelastic scattering events several secondary electrons which form the basis for the conductivity of the atmosphere. As in the Karzas-Latter approach, each Compton electron is assumed to have a constant speed, V_0 , throughout the range, R , of the electron which is a function of altitude. This allows the lifetime to be expressed as R/V_0 . If each Compton electron produces secondary electrons at a constant rate, the rate of secondary electron, n_s , production is

$$\frac{dn_s}{dt} = \frac{E_c/33 \text{ eV}}{R/V_0} n_c \quad (5)$$

where E_c is the energy of the Compton electron and 33 eV is the average ionization energy per air molecule (Ref 2).

Considering the differential current produced by the Compton electrons, it can be shown (Ref 3) that the Compton current and the number of Compton electrons are given by

$$\vec{j}^c(\tau) = -e g(r) \int_0^{R/V_0} v(\tau') f\left(\tau - \tau' + \frac{x(\tau')}{c}\right) d\tau' \quad (6)$$

$$n_c(\tau) = g(r) \int_0^{R/V_0} f\left(\tau - \tau' + \frac{x(\tau')}{c}\right) d\tau' \quad (7)$$

where

$$\tau = t - \frac{r}{c}$$

τ' = the time since the creation of the Compton electron

$X(\tau')$ = the radial distance the Compton electron has traveled

e = the magnitude of the electron charge

The quantity τ is generally known as retarded time.

It then follows from Eqs (4) and (7) that the number of secondary electrons is

$$n_s(\tau) = \frac{qV_0}{R} g(r) \int_{-\infty}^{\tau} \left[\int_0^{R/V_0} f\left(\tau' - \tau'' + \frac{X(\tau'')}{c}\right) d\tau'' \right] d\tau' \quad (8)$$

where q is $E_C/33$ eV.

Currents and Conductivity

In the Karzas-Latter theory, the speed of the Compton electrons is considered to be a constant, however, there is an acceleration due to the geomagnetic field. The general equation of motion for an electron in this case is

$$\frac{d}{dt} m \gamma \vec{v} = -e (\vec{E} + \vec{v} \times \vec{B}) - m v_c \vec{v} \quad (9)$$

where

m = the electron rest mass

\vec{v} = the electron velocity

\vec{E} = the electric field

\vec{B} = the magnetic field

v_c = the electron collision frequency

$$\gamma = (1 - (v_0/c)^2)^{-\frac{1}{2}}$$

If the relativistic motion of the electron is considered, only the $V \times B$ term is important and in spherical coordinates, the expressions for the velocity components become (Ref 3)

$$V_r = V_0 (\sin^2 \theta \cos \omega t + \cos^2 \theta) \quad (10)$$

$$V_\theta = V_0 (\cos \theta \sin \theta \cos \omega t - \sin \theta \cos \theta) \quad (11)$$

$$V_\phi = V_0 (\sin \theta \sin \omega t) \quad (12)$$

where ω is the cyclotron frequency for an electron and is given by

$$\omega = \frac{eB_0}{m\gamma} \quad (13)$$

with B_0 the magnitude of the geomagnetic field.

From Eq (10), $X(\tau')$ is found to be

$$X(\tau') = V_0 \left(\sin^2 \theta \frac{\sin \omega \tau'}{\omega} + \tau' \cos^2 \theta \right) \quad (14)$$

The Compton currents may now be written as

$$J_r^C(\tau) = -eg(r) V_0 \int_0^{R/V_0} [f(T) (\cos^2 \theta + \sin^2 \theta \cos \omega T)] d\tau' \quad (15)$$

$$J_\theta^C(\tau) = -eg(r) V_0 \int_0^{R/V_0} [f(T) \sin \theta \cos \theta (\cos \omega T - 1)] d\tau' \quad (16)$$

$$J_\phi^C(\tau) = -eg(r) V_0 \int_0^{R/V_0} [f(T) \sin \theta \sin \omega T] d\tau' \quad (17)$$

where

$$T = \tau - \left(1 - \frac{V_0}{c} \cos^2 \theta\right) \tau' + \frac{V_0}{c} \sin^2 \theta \frac{\sin \omega \tau'}{\omega} \quad (18)$$

In a similar manner Eq (8) becomes

$$n_s(\tau) = \frac{qV_0}{R} g(r) \int_{-\infty}^T \left[\int_0^{R/V_0} f(\tau') d\tau' \right] d\tau' \quad (19)$$

where

$$T' = \tau' - \left(1 - \frac{V_0}{c} \cos^2 \theta\right) \tau'' + \frac{V_0}{c} \sin^2 \theta \frac{\sin \omega \tau''}{\omega} \quad (20)$$

Equations (15), (16), (17), (18), and (20) may be simplified if the factor $\omega \tau$ is assumed to be small. In this case a Taylor series expansion for the sin and cos of $\omega \tau$, including only first and second order terms, is

$$\sin \omega \tau = \omega \tau \quad (21)$$

$$\cos \omega \tau = 1 - \frac{\omega^2 \tau^2}{2} \quad (22)$$

The expressions for the Compton currents now become

$$J_r^C(\tau) = -eg(r) V_0 \left[\int_0^{R/V_0} f(\tau) d\tau - \sin^2 \theta \frac{\omega^2}{2} \int_0^{R/V_0} \tau'^2 f(\tau) d\tau' \right] \quad (23)$$

$$J_\theta^C(\tau) = eg(r) V_0 \sin \theta \cos \theta \frac{\omega^2}{2} \int_0^{R/V_0} \tau'^2 f(\tau) d\tau' \quad (24)$$

$$J_g^C(\tau) = -eg(r) V_0 \sin \theta \omega \int_0^{R/V_0} \tau' f(\tau) d\tau' \quad (25)$$

$$T = \tau - (1 - \beta) \tau' \quad (26)$$

where $\beta = \frac{V_0}{c}$.

In a like manner Eq (20) becomes

$$\tau' = \tau - (1 - \beta) \tau'' \quad (27)$$

An expression for the conductivity may also be found by using the equation of motion for the secondary electrons. These electrons are in the thermal regions with energies ranging from about 10-15 eV to the ambient energy. It should be remembered for later use that the ambient energy of the secondary electrons is dependent on the electric field present. For consideration here, it is assumed that $\gamma \approx 1$ and also that the change of velocity with time is small compared to the other terms in Eq (9) so that $\frac{d\vec{V}}{dt}$ may be neglected. Also, with low velocities, the $\vec{V} \times \vec{B}$ term is small compared to the remaining terms and may also be neglected. Then the velocity of the secondary electrons is

$$\vec{V} = - \frac{e}{mv_c} E \quad (28)$$

Using Eq (28), the current due to the secondary electrons is

$$\vec{J}^S(\tau) = - e \vec{V} n_S(\tau) = \frac{e^2}{mv_c} \vec{E} n_S(\tau) \quad (29)$$

Comparing Eq (29) to $\vec{J}^S = \sigma \vec{E}$, an expression for the conductivity

is

$$\sigma(\tau) = \frac{e^2}{mv_c} n_S(\tau) \quad (30)$$

Equations (19), (23), (24), (25), (26), (27), and (30) provide the desired expressions for the Compton currents and the conductivity.

Field Equations

Maxwell's equations in rationalized MKS units are

$$\vec{\nabla} \times \vec{E} = - \frac{\partial \vec{B}}{\partial t} \quad (31)$$

$$\vec{\nabla} \times \vec{B} = \mu_0 \vec{J} + \frac{1}{c^2} \frac{\partial \vec{E}}{\partial t} \quad (32)$$

$$\vec{\nabla} \cdot \vec{E} = \frac{q_v}{\epsilon_0} \quad (33)$$

$$\vec{\nabla} \cdot \vec{B} = 0 \quad (34)$$

where q_v is the total charge density and \vec{J} is the total current density.

In addition to these equations the continuity of charge requires that

$$\frac{\partial q_v}{\partial t} + \vec{\nabla} \cdot \vec{J} = 0 \quad (35)$$

Combining these equations to separate \vec{E} and \vec{B} and transforming them into spherical coordinates and into the retarded time frame (Ref 3) the relations for \vec{E} and \vec{B} become

$$- \nabla^2 \vec{E} + \hat{u}_r \frac{1}{c\epsilon_0} \vec{\nabla} \cdot \vec{J} + \frac{1}{\epsilon_0} \vec{\nabla} q_v \quad (36)$$

$$+ \frac{\partial}{\partial t} \left[\frac{2}{c} \frac{1}{r} \frac{\partial}{\partial r} (r\vec{E}) + \mu_0 (\vec{J} - \hat{u}_r J_r) \right] = 0$$

$$- \nabla^2 \vec{B} - \mu_0 \vec{\nabla} \times \vec{J} + \frac{\partial}{\partial t} \left[\frac{2}{rc} \frac{\partial}{\partial r} (r\vec{B}) \right. \quad (37)$$

$$\left. + \frac{\mu_0}{c} (\hat{u}_\theta J_\phi - \hat{u}_\phi J_\theta) \right] = 0$$

In the Karzas-Latter model, only the time derivative portion of Eqs (36) and (37) are kept since the current variation with distance is slow compared to the variation in time for the high frequency com-

ponents. Also the fields and currents vary rapidly in time. This approximation is valid for about 100 shakes. The same high frequency approximation is used here. In addition, the radial component of the field is dropped since it is weak compared to the transverse components and contributes only a very low frequency signal (Ref 2). The equations for the transverse components are

$$\frac{\partial}{\partial \tau} \left[\frac{2}{c} \frac{1}{r} \frac{\partial}{\partial r} (r E_{\theta, \vartheta}) + \mu_0 J_{\theta, \vartheta} \right] = 0 \quad (38)$$

$$\frac{\partial}{\partial \tau} \left[\frac{2}{c} \frac{1}{r} \frac{\partial}{\partial r} (r B_{\theta}) - \frac{\mu_0}{c} J_{\vartheta} \right] = 0 \quad (39)$$

$$\frac{\partial}{\partial \tau} \left[\frac{2}{c} \frac{1}{r} \frac{\partial}{\partial r} (r B_{\vartheta}) + \frac{\mu_0}{c} J_{\theta} \right] = 0 \quad (40)$$

The currents in Eqs (38), (39), and (40) are total currents. The total currents are given by

$$J_{\theta, \vartheta} = J_{\theta, \vartheta}^C + \sigma(\tau) E_{\theta, \vartheta} \quad (41)$$

Substitution of Eq (41) into Eqs (38), (39), and (40) and integration over time gives

$$\frac{2}{c} \frac{1}{r} \frac{\partial}{\partial r} (r E_{\theta}) + \mu_0 J_{\theta}^C + \mu_0 \sigma(\tau) E_{\theta} = 0 \quad (42)$$

$$\frac{2}{c} \frac{1}{r} \frac{\partial}{\partial r} (r E_{\vartheta}) + \mu_0 J_{\vartheta}^C + \mu_0 \sigma(\tau) E_{\vartheta} = 0 \quad (43)$$

$$\frac{2}{c} \frac{1}{r} \frac{\partial}{\partial r} (r B_{\theta}) - \frac{\mu_0}{c} J_{\vartheta}^C - \frac{\mu_0}{c} \sigma(\tau) E_{\vartheta} = 0 \quad (44)$$

$$\frac{2}{c} \frac{1}{r} \frac{\partial}{\partial r} (r B_{\vartheta}) + \frac{\mu_0}{c} J_{\theta}^C + \frac{\mu_0}{c} \sigma(\tau) E_{\theta} = 0 \quad (45)$$

Equations (42) and (43) are in a form which can be solved. The terms needed for solution of these equations are the air conductivity and the transverse components of the Compton currents. The air conductivity may be found by using Eqs (19) and (30). The transverse components of the Compton currents may be found by using Eqs (24) and (25).

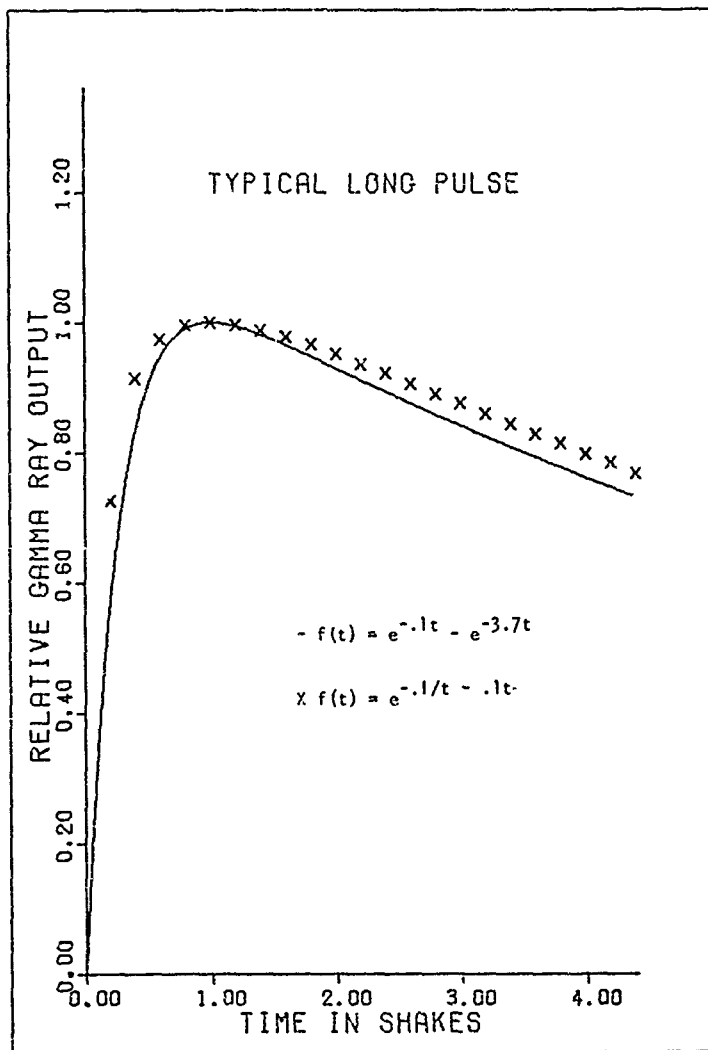


Fig. 2. Typical Long Gamma Output Pulse

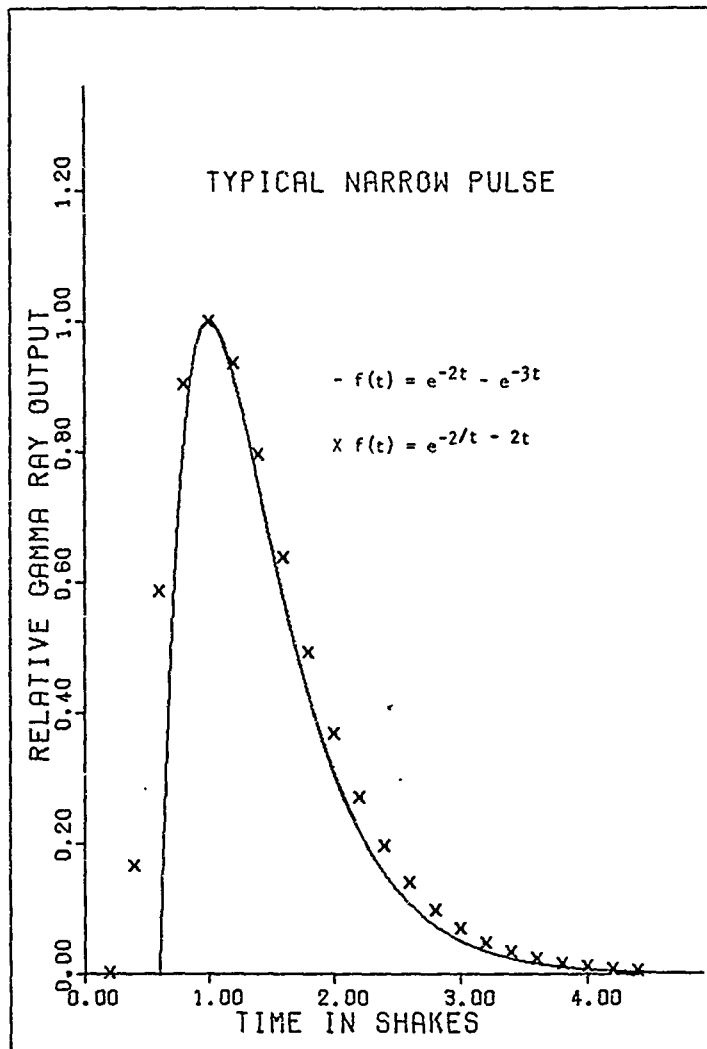


Fig. 3. Typical Narrow Gamma Output Pulse

IV. Results

To test the validity of the HAEMP model, the computed values of this model were compared to available equivalent model values from the AFWL code for EMP calculations known as CHEMP (Ref 4).

The basic set of conditions used for these calculations was:

target location	= ground zero
height of burst	= 100 Km
geomagnetic field	= .3 gauss or $3 (10)^{-5}$ wb/m ²
inclination angle	= 0.6 degree
Compton electron recoil energy	= .75 MeV

The gamma yield was varied and the number of steps taken for the numerical integration was varied according to the gamma yield, with more steps taken for the higher yields. Other parameters varied for examination of peak field values were burst height, geomagnetic field, and pulse shape. A preionization level was also considered.

The available data from the CHEMP(N) code, which is CHEMP run with non-self-consistent calculations, was computed using a pulse of the form of Eq (46) with $\alpha = 10^{-9}$ and $\beta = 10^7$ and the same geometry as given above. This pulse shape is almost identical to that of Eq (48) with $\alpha = 10^7$ and $\beta = 3.7 (10)^8$. See Fig. 2 on page 18. Using this pulse shape, a range of gamma yields from .01 Kt to 100 Kt was used to calculate the EMP field values. The peak field values are plotted in Fig. 4. The values taken from the CHEMP(N) code are annotated by X marks. These peak field values show a maximum difference of 5.5% around the 1 Kt case, and a difference of less than 2% for all other known cases.

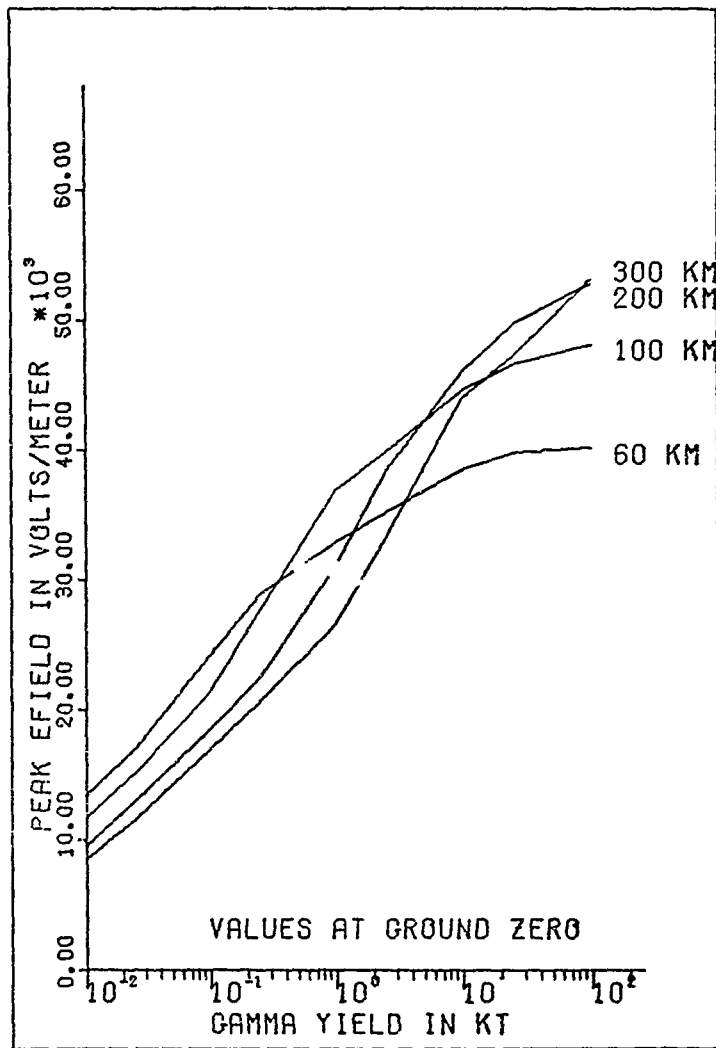


Fig. 6. Peak Electric Field as a Function of Burst Height

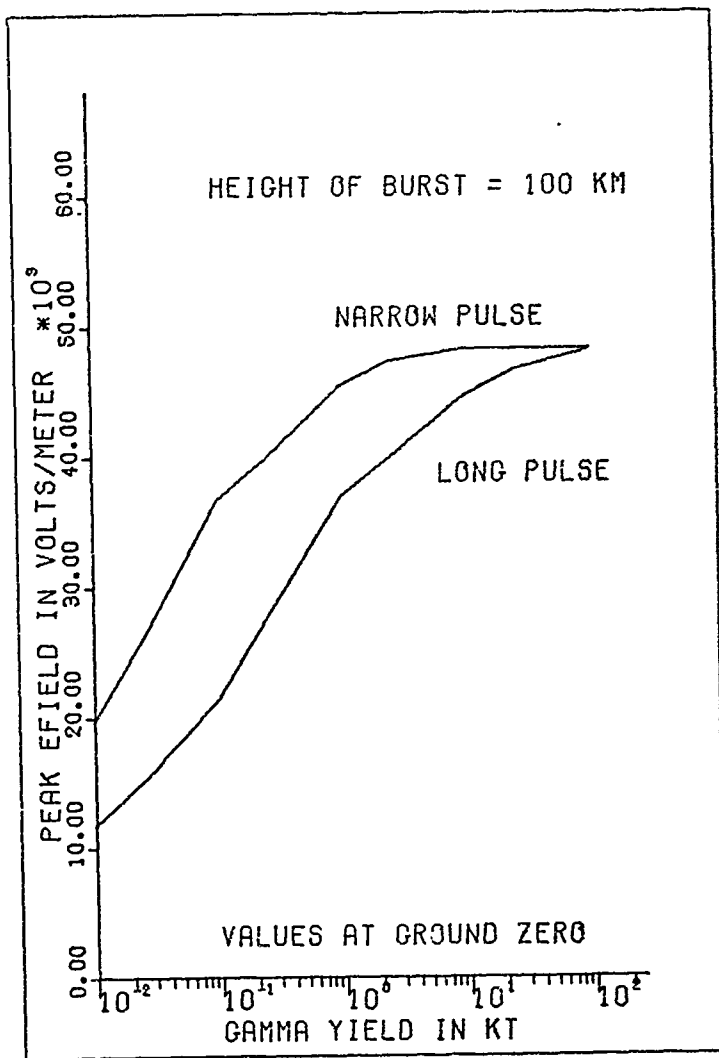


Fig. 7. Peak Electric Fields for Two Gamma Pulse Shapes

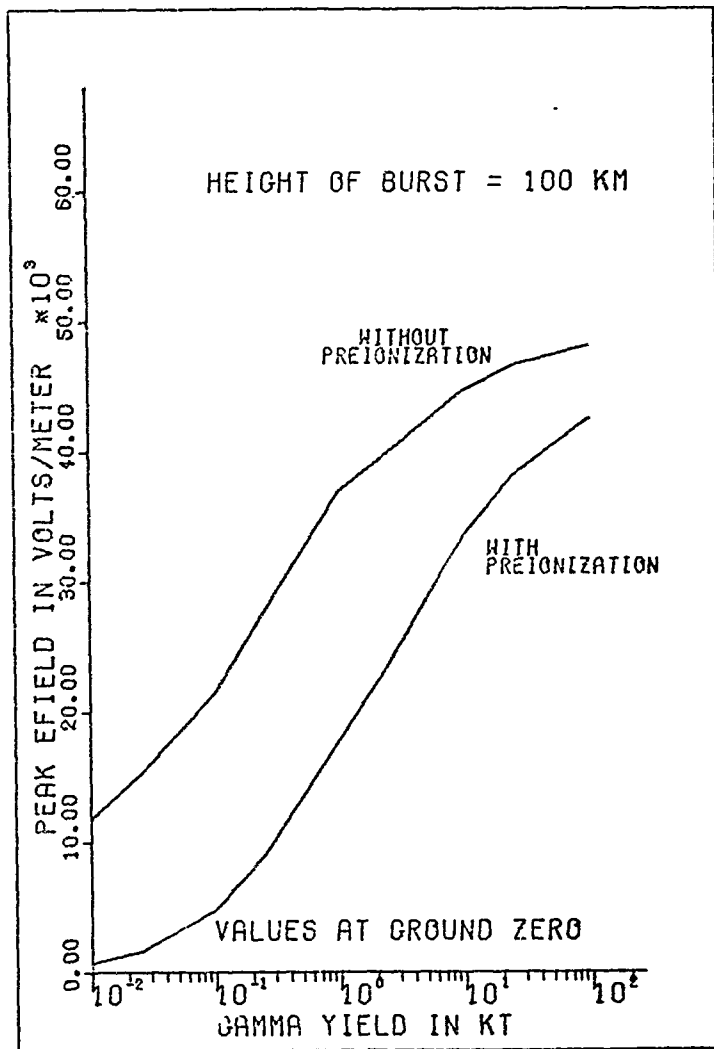


Fig. 8. Effect of a .03 Kt Gamma Yield Precursor Burst

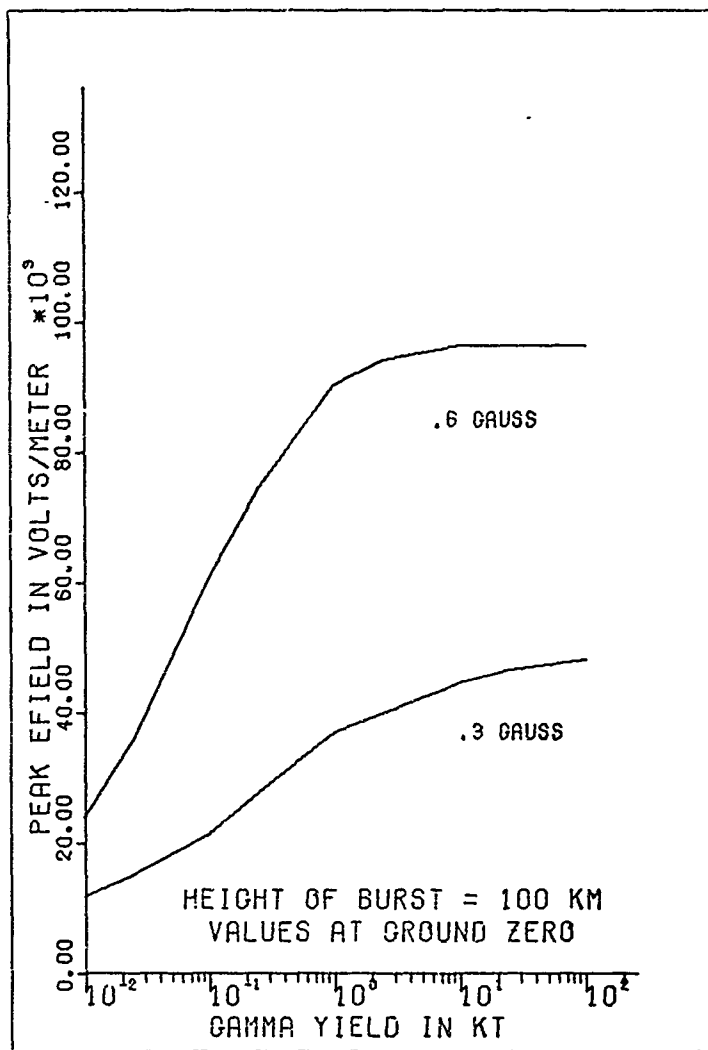


Fig. 9. Effect of Geomagnetic Field Strength on Peak Fields

Bibliography

1. Kinsley, O.V. Introduction to the Electromagnetic Pulse, Wright-Patterson AFB: Air Force Institute of Technology, March 1971. (GNE/PH/71-4).
2. Karzas, W.J. and R. Latter. "Detection of the Electromagnetic Radiation from Nuclear Explosions in Space", Physical Review, 137-5B:1369-1378 (March 8, 1965).
3. Chapman, T.C. A Computer Code for High Altitude EMP, Wright-Patterson AFB: Air Force Institute of Technology, January 1974. (GNE/PH/74-1).
4. Canavan, G.H., J.E. Brau, L.A. Wittwer. Sensitivity of Self-Consistent High Altitude Electromagnetic Pulse Calculations to Pre-ionization and Improved Source and Ionization Models. AFWL EMP Theoretical Note 190. Kirtland AFB: Air Force Weapons Laboratory, October 1973.
5. Pomraning, G.C. "Early Time Air Fireball Model for a Near-Surface Burst", DWA 3029T, March 1973.
6. Evans, R.D. The Atomic Nucleus, New York: McGraw Hill Book Co. 1966.
7. Katz, L. and A.S. Penfold. "Range-Energy Relations for Electrons and the Determination of Beta-Ray End-Point Energies by Absorption", Reviews of Modern Physics, 24-1:28-44 (January 1952).
8. Latter, R. and R.E. Lelevier. "Detection of Ionization Effects from Nuclear Explosions in Space", Journal of Geophysical Research, 68-6 (March 15, 1963)
9. Air Force Weapons Laboratory. CHEMP: A Code for Calculation of High-Altitude EMP. AFWL Technical Report 74-49. Kirtland AFB: AFWL, July 1974.
10. Baum, C.E. Electron Thermalization and Mobility in Air. AFWL EMP Theoretical Note 12 (AFWL-EMP 2-1). Kirtland AFB: Air Force Weapons Laboratory, July 1965.
11. U.S. Standard Atmosphere, 1962. Washington DC: U.S. Government Printing Office. December 1962.
12. Carnahan, B., H.A. Luther, J.O. Wilkes. Applied Numerical Methods, New York: John Wiley & Sons, Inc. 1969.